The neurexin ligands, neuroligins and leucine-rich repeat transmembrane proteins, perform convergent and divergent synaptic functions in vivo

Gilberto J. Soler-Llavina[a,1], Marc V. Fuccillo[a,b,1], Jaewon Ko[b,2], Thomas C. Südhof[b,c], and Robert C. Malenka[a,3]

[a]Nancy Pritzker Laboratory, Department of Psychiatry and Behavioral Sciences, [b]Department of Molecular and Cellular Physiology, [c]Howard Hughes Medical Institute, Stanford University School of Medicine, Stanford, CA 94305-5453

This contribution is part of the special series of Inaugural Articles by members of the National Academy of Sciences elected in 2011.

Contributed by Robert C. Malenka, August 25, 2011 (sent for review August 2, 2011)

Synaptic cell adhesion molecules, including the neurexin ligands, neuroligins (NLs) and leucine-rich repeat transmembrane proteins (LRRTMs), are thought to organize synapse assembly and specify synapse function. To test the synaptic role of these molecules in vivo, we performed lentivirally mediated knockdown of NL3, LRRTM1, and LRRTM2 in CA1 pyramidal cells of WT and NL1 KO mice at postnatal day (P)0 (when synapses are forming) and P21 (when synapses are largely mature). P0 knockdown of NL3 in WT or NL1 KO neurons did not affect excitatory synaptic transmission, whereas P0 knockdown of LRRTM1 and LRRTM2 selectively reduced AMPA receptor-mediated synaptic currents. P0 triple knockdown of NL3 and both LRRTMs in NL1 KO mice yielded greater reductions in AMPA and NMDA receptor-mediated currents, suggesting functional redundancy between NLs and LRRTMs during early synapse development. In contrast, P21 knockdown of LRRTMs did not alter excitatory transmission, whereas NL manipulations supported a role for NL1 in maintaining NMDA receptor-mediated transmission. These results show that neurexin ligands in vivo form a dynamic synaptic cell adhesion network, with compensation between NLs and LRRTMs during early synapse development and functional divergence upon synapse maturation.

hippocampus | neuropsychiatric disorders

The enormous processing power of the mammalian brain is the result of a vast network of precise synaptic connections, where functionally diverse presynaptic neurons establish synapses with specific properties onto select populations of postsynaptic cells. Neuroligins (NLs) and neurexins (NRXs) are a prototypical transsynaptic adhesion pair (1, 2) that is ideally situated to play important roles in such synaptic processes. Interactions between the four NLs (NL1–4) and the three NRXs are highly regulated at the level of alternative mRNA splicing, generating an intricate code that regulates both the affinity of interactions and the consequences on synapse specification (3, 4). Given the complexity of NL–NRX interactions, it was surprising to find that leucine-rich repeat transmembrane proteins (LRRTMs) are also high-affinity receptors for NRXs and share many of the binding characteristics of NLs (5–7).

Functional studies of NLs and LRRTMs using overexpression in nonneuronal cells or cultured neurons showed that increases in the levels of these proteins generally increase the number of synapses (5, 8–12). Loss of function experiments aiming to address the requirement for NLs and LRRTMs in synapse formation and mature synaptic function have yielded inconsistent results depending on whether KO or knockdown (KD) approaches were used (6, 9–15). These discrepancies may reflect, in part, inherent differences between the preparations that were used. In particular, robust ongoing synaptogenesis in dissociated cultures and extensive circuit remodeling in slice culture preparations make it difficult to distinguish whether a manipulation affects synapse formation, synapse pruning, synapse maintenance, or mature synaptic function. In vivo approaches are similarly challenging. Constitutive mouse KOs that are currently used for analysis of NLs and NRXs (10, 13, 16) provide no temporal control of gene ablation, and circuit-level reorganization or compensatory mechanisms (17) can obscure potential phenotypes [although the fact that the triple NL KO mice and the triple αNRX mice exhibit lethal impairments in synaptic transmission (13, 16) argues against complete compensation of the function of these deleted NL and NRX genes]. To circumvent some of the limitations of traditional in vitro and in vivo preparations, we have now used stereotactically guided injections of lentiviral-mediated shRNAs into the hippocampal CA1 region, thus creating a neuronal mosaic that is advantageous for analyzing the effects of postsynaptic molecular manipulations on basal excitatory synaptic transmission. The use of lentiviruses capable of expressing up to three shRNAs simultaneously (18) allowed the study of the individual and combined functions of NLs and LRRTMs in an intact hippocampal circuit at two developmental periods: during ongoing synaptogenesis and when synapses had fully matured.

Our data suggest that in vivo, LRRTMs and NLs are part of a functionally dynamic cell adhesion network that regulates excitatory synaptic transmission. KD of NLs and LRRTMs alone or together reveals that these proteins redundantly contribute to maintain synaptic function during early hippocampal development. However, NLs and LRRTMs perform divergent functions after synaptogenesis. Taken together, our data suggest that, as synaptic cell adhesion molecules, NLs and LRRTMs function in a manner dependent on developmental stage to regulate synaptic strength in vivo.

Results

KD of NL3, LRRTM1, and LRRTM2 During Synaptogenesis in Vivo. To test our approach for examining the in vivo function of cell adhesion proteins during new synapse formation, we stereotactically injected lentiviruses expressing GFP into the hippocampus of P0 WT mice, resulting in specific targeting of the CA1 region with no detectable infection of the nearby CA3 region or dentate gyrus (Fig. S1*A*). We then prepared acute hippocampal slices from these animals at P14–P18 and examined basal properties of Schaffer collateral to CA1 pyramidal neuron synapses using simultaneous whole-cell recordings from neighboring infected and uninfected cell pairs (Fig. S1). The use of paired recordings to study basal synaptic strength assumes that roughly equal numbers of synapses are activated on adjacent infected and uninfected cells when a single stimulus to the Schaffer collaterals is applied; thus, the evoked excitatory postsynaptic currents (EPSCs) will be of similar amplitudes. Control measurements of α-amino-3-hydroxy-5-methyl-4-isoxazolepropionic acid receptor (AMPAR)-

Author contributions: G.J.S.-L., M.V.F., J.K., T.C.S., and R.C.M. designed research; G.J.S.-L. and M.V.F. performed research; G.J.S.-L. and M.V.F. analyzed data; and G.J.S.-L., M.V.F., T.C.S., and R.C.M. wrote the paper.

The authors declare no conflict of interest.

[1]G.J.S.-L. and M.V.F. contributed equally to this work.

[2]Present address: Department of Biochemistry, College of Life Science and Biotechnology, Yonsei University, Seoul 120-749, South Korea.

[3]To whom correspondence should be addressed. E-mail: malenka@stanford.edu.

This article contains supporting information online at www.pnas.org/lookup/suppl/doi:10.1073/pnas.1114028108/-/DCSupplemental.

mediated EPSCs at −60 mV (AMPAR EPSCs) and N-methyl D-aspartate receptor (NMDAR)-mediated EPSCs at +40 mV (NMDAR EPSCs; measured 50 ms after the stimulus) confirmed this assumption (Fig. S1*B*), revealing a strong correlation in EPSC amplitudes between cell pairs, one of which expressed GFP. We also examined paired pulse ratios (PPRs) at different interstimulus intervals (ISIs). PPR was not different between pairs at any ISI (Fig. S1*C*), which would be expected from cells sharing common inputs. These results confirm that the viral manipulation is exclusive to CA1 neurons and that our assay will likely detect any changes in synapse number and/or function caused by the in vivo molecular manipulations.

To examine the functions of NL1, NL3, LRRTM1, and LRRTM2, which are highly expressed in hippocampal CA1 pyramidal cells during late embryogenesis and continuing into the adult (19, 20), we stereotactically injected lentiviruses expressing shRNAs targeting NL3 or LRRTM1 and LRRTM2 [NL3 KD or LRRTM double knockdown (DKD)] (ref. 18 has validation of the effectiveness, lack of off-target effects, and specificity of these shRNAs) into the hippocampus of P0 WT or NL1 KO mice. We focused specifically on NL1 and NL3, because these isoforms are expressed at glutamatergic synapses (19, 21, 22). In slices prepared from P14 to P18 WT mice, NL3 KD (Fig. 1*A*) yielded, on average, no change in either AMPAR EPSCs (Fig. 1 *A2* and *A4*) (NL3 KD = 123.6 ± 12.9 pA; WT = 122.1 ± 12.6 pA; NL3 KD = 1.01 ± 0.11 of WT) or NMDAR EPSCs (Fig. 1 *A3* and *A4*) (NL3 KD = 64.3 ± 9.5 pA; WT = 68.9 ± 9.3 pA; NL3 KD = 0.93 ± 0.14 of WT). To assess whether NL1 could be compensating for the loss of NL3, we injected NL3 KD virus into NL1 KO mice, thereby creating synapses deficient for both NLs (termed NL1/3 Def) (Fig. 1*B*). Similar to the NL3 KD alone, NL1/3 Def cells exhibited no net change in either AMPAR EPSCs (Fig. 1 *B2* and *B4*) (NL1/3 Def = 109.7 ± 10.6 pA; NL1 KO = 112.5 ± 13.4 pA; NL1/3 Def = 0.97 ± 0.09 of NL1 KO) or NMDAR EPSCs (Fig. 2 *B3* and *B4*) (NL1/3 Def = 80.4 ± 11.9 pA; NL1 KO = 83.1 ± 9.2 pA; NL1/3 Def = 0.97 ± 0.14 of NL1 KO) compared with adjacent NL1 KO cells. To interpret these results, it is essential to know whether the NL1 KO cells exhibit any synaptic phenotype compared with WT cells at this age. Because a constitutive KO in which all cells lack NL1 precludes a separate analysis of AMPAR- and NMDAR-mediated transmission with paired recordings, we relied on NMDAR/AMPAR EPSC ratios to uncover differences between NL1 KO and WT cells. Surprisingly and different from later developmental time points (10), at P14–18, NL1 KO neurons exhibited NMDAR/AMPAR ratios similar to WT littermate controls. The relative contributions of AMPAR- and NMDAR-mediated transmission remained unaltered across all NL manipulations, which was evidenced by the consistency of NMDAR/AMPAR ratios (Fig. 1*C*) (WT = 0.47 ± 0.03; NL1 KO = 0.48 ± 0.03; NL3 KD = 0.52 ± 0.04; NL1/3 Def = 0.46 ± 0.03).

Although we observed no change in the total amount of NMDAR-mediated current in NL1/3 Def cells, it is possible that NL1 and NL3 manipulations alter the subunit composition of synaptic NMDARs, a property that is developmentally regulated (23). To address this possibility, we analyzed the weighted decay time constant (τ_W) of the compound EPSCs recorded at +40 mV (Fig. 1*D*), because the time course of NMDAR EPSCs is significantly influenced by NMDAR subunit composition (24). The τ_W for both NL1 KO and NL1/3 Def EPSCs was no different from the τ_W of WT EPSCs (WT = 108.5 ± 5.7 ms; NL1 KO = 106.7 ± 6.5 ms; NL1/3 Def = 112.1 ± 9.0 ms), suggesting that NL1 and NL3 do not regulate synaptic NMDAR subunit composition during this early postnatal time period. To assess whether removal of NL1 and NL3 alters presynaptic function during synaptogenesis in vivo, we compared the PPR at multiple ISIs across all four genotypes (Fig. 1*E*). No differences were noted between any of the genotypes, suggesting that NL1 and NL3 are not required for the regulation of presynaptic properties during the first 2 postnatal wk.

LRRTM1–LRRTM4 were recently identified as high-affinity NRX ligands that share many binding characteristics with NLs, including their calcium and splice site dependence (5–7). LRRTM1 and LRRTM2 are the major LRRTMs expressed within CA1 pyramidal cells (20). To address their synaptic

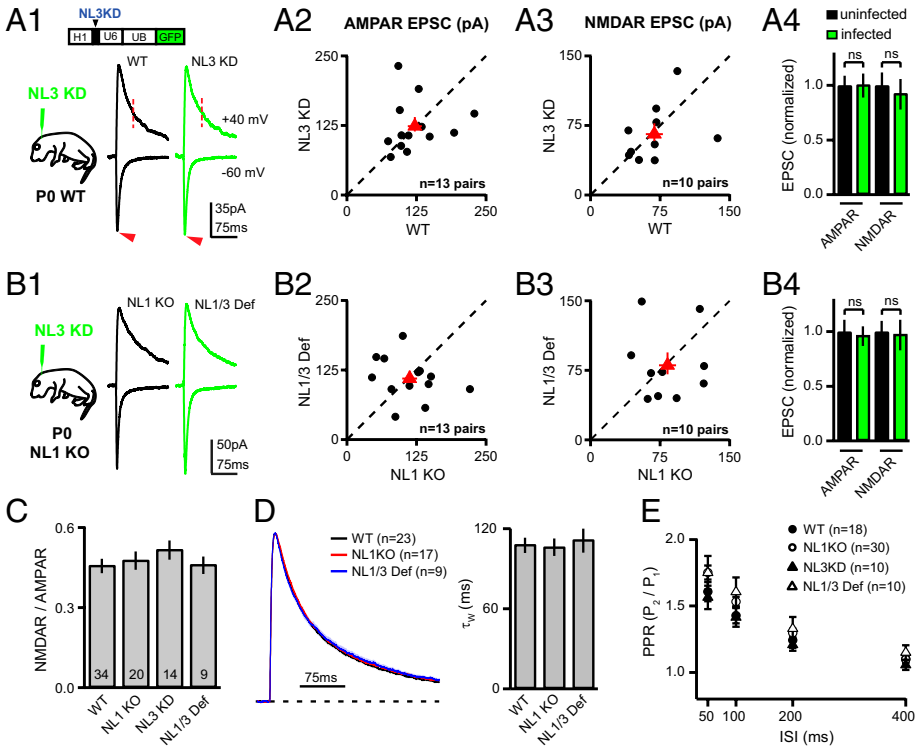

Fig. 1. Neuroligins are not required for normal development of basal excitatory synaptic transmission in hippocampal CA1 pyramidal neurons. (*A1*) Schematic of vector for KD of NL3 in P0 WT mice and representative traces of EPSCs at −60 and +40 mV simultaneously recorded from an uninfected control cell (black) and an infected, GFP-expressing cell (green). All subsequent panels where this diagram appears are represented in the same manner. In black, the mouse's genotype and age are shown, and in green the lentivirus injected is shown. (*A2* and *A3*) Amplitude of AMPAR and NMDAR EPSCs (measured where indicated by arrowheads and dotted lines in *A1*, respectively) of infected cells plotted against the amplitudes of simultaneously recorded uninfected controls (black circles) and the average EPSC amplitude (red triangle). (*A4*) Summary graph of AMPAR and NMDAR EPSCs normalized to the average EPSC amplitude of each corresponding uninfected control. (*B1–B4*) The same as in *A1–A4* for experiments performed in NL1 KO mice. (*C*) Summary graph of the NMDAR/AMPAR ratios for the indicated genotypes. Numbers within each bar represent *n*. (*D Left*) Average normalized EPSCs recorded at +40 mV from WT (black), NL1KO (red), and NL1/3 Def (blue) neurons. Solid lines are averages across multiple cells (indicated by the numbers in parentheses), and shaded areas represent the SEM. (*D Right*) Summary of the weighted decay time constant obtained from double exponential fits to each individual experiment. (*E*) Summary of PPRs measured at four different ISIs for each of the indicated genotypes. All summary values are presented as mean ± SEM.

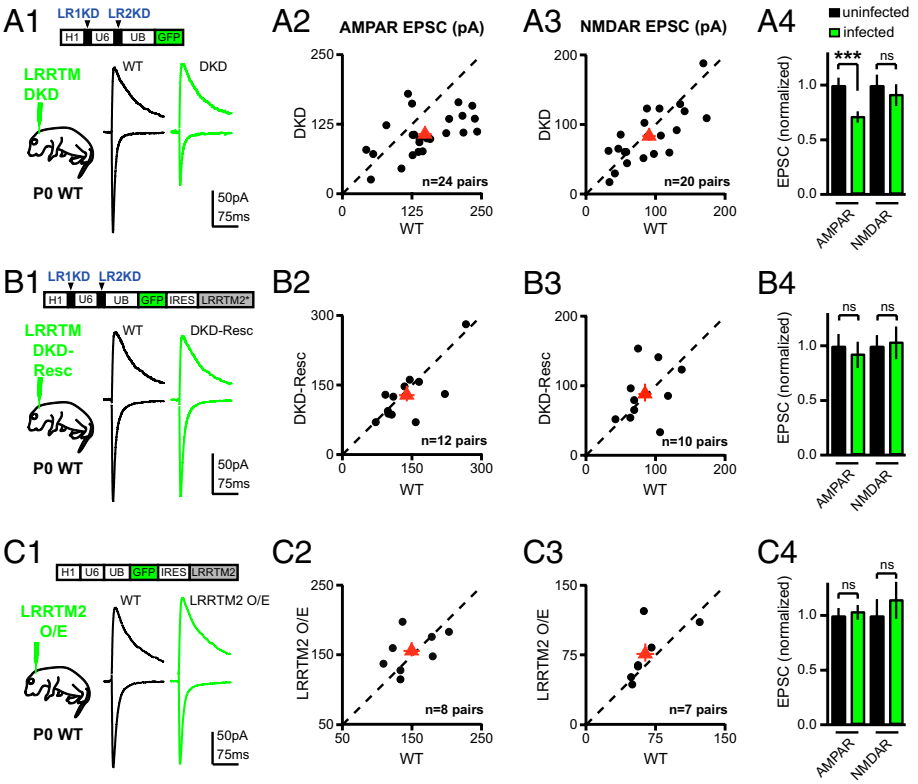

Fig. 2. Double KD of LRRTM1 and -2 during synaptogenesis in vivo selectively impairs AMPAR-mediated transmission. (*A1*) Schematic of vector for DKD of LRRTMs in P0 WT mice and representative traces of EPSCs at −60 and +40 mV simultaneously recorded from an uninfected control cell (black) and an infected GFP-expressing cell (green). (*A2* and *A3*) Amplitude of AMPAR and NMDAR EPSCs of infected cells plotted against the amplitudes of simultaneously recorded uninfected controls (black circles) and the average EPSC amplitude (red triangle). (*A4*) Summary graph of AMPAR and NMDAR EPSCs normalized to the average EPSC amplitude of each corresponding uninfected control. (*B* and *C*) The same as in *A* for experiments performed using the LRRTM DKD + Rescue and LRRTM2 O/E constructs, respectively. All summary values are presented as mean ± SEM. ***$P < 0.001$.

function during synaptogenesis in vivo, we knocked down both LRRTMs in P0 WT mice (DKD) (Fig. 2*A1*). Paired comparisons of LRRTM DKD with adjacent WT neurons revealed a significant decrease in AMPAR EPSCs (Fig. 2 *A2* and *A4*) (LRRTM DKD = 107.2 ± 7.7 pA; WT = 148.2 ± 12 pA; LRRTM DKD = 0.72 ± 0.05 of WT) but no change in NMDAR EPSCs (Fig. 2 *A3* and *A4*) (LRRTM DKD = 83.2 ± 9.0 pA; WT = 90.4 ± 9.8 pA; LRRTM DKD = 0.92 ± 0.1 of WT). These data suggest that LRRTMs participate in regulating AMPAR-mediated transmission at CA1 pyramidal cell synapses during the first 2 postnatal wk. Consistent with data obtained in cultured neurons (18), the lack of effect of the LRRTM DKD on NMDAR EPSCs also suggests that this manipulation did not alter total synapse numbers, because this finding would be expected to reduce both AMPAR- and NMDAR-mediated currents to the same extent.

To determine if the decrease in AMPAR EPSCs was, in fact, because of the KD of LRRTMs rather than an off-target effect of the shRNAs, we tested whether reintroducing WT LRRTM2 could reverse the phenotype (Fig. 2*B1*). An shRNA-insensitive version of LRRTM2, expressed bicistronically after EGFP from an internal ribosomal entry site (IRES) (DKD-Rescue), indeed reversed the deficit in AMPAR-mediated transmission (Fig. 2 *B2* and *B4*) (DKD-Rescue = 128.4 ± 16.8; WT = 138.8 ± 16.5; DKD-Rescue = 0.93 ± 0.12 of WT), whereas NMDAR EPSCs were unchanged (Fig. 2 *B3* and *B4*) (DKD-Rescue = 88.4 ± 12.7 pA; WT = 84.8 ± 9.4 pA; DKD-Rescue = 1.04 ± 0.15 of WT). These results suggest that, during synapse formation and stabilization, LRRTMs play a role in recruiting and/or maintaining synaptic AMPARs.

If LRRTMs alone are sufficient for this activity, overexpression of WT LRRTM2 at P0 may increase AMPAR-mediated synaptic transmission without altering NMDAR-mediated currents. To test this hypothesis, we injected a lentivirus that expressed WT LRRTM2 [LRRTM2 overexpression (O/E)] (Fig. 2*C1*) into the CA1 layer of WT P0 mice. Surprisingly, comparison of WT and LRRTM2 O/E cells showed no changes in AMPAR currents (Fig. 2 *C2* and *C4*) (LRRTM2 O/E = 155.4 ± 10.2 pA; WT = 149.4 ± 11.7 pA; LRRTM2 O/E = 1.04 ± 0.07 of WT). As predicted, NMDAR EPSCs were also unchanged (LRRTM2 O/E = 76.0 ± 9.8 pA; WT = 61.9 ± 9.6 pA; LRRTM2 O/E = 1.2 ± 0.16 of WT). These results suggest that LRRTM2 alone is not sufficient to increase the incorporation and maintenance of synaptic AMPARs in vivo or that native levels of LRRTMs are saturating for these processes. Furthermore, they suggest that overexpression of LRRTM2 in vivo does not have the same robust synaptogenic effect as this manipulation has in vitro.

NLs and LRRTMs Function Cooperatively at Developing CA1 Synapses in Vivo. Given the high affinity of both NLs and LRRTMs for NRXs, it is possible that, in the absence of one family of NRX ligands, the other family can functionally compensate. To test whether these NRX ligands exhibit overlap in their synaptic functions in vivo, we injected NL1 KO pups with a lentivirus that expressed shRNAs to LRRTM1, LRRTM2, and NL3, thereby creating synapses deficient for NL1, NL3, LRRTM1, and LRRTM2 [triple knockdown (TKD)/KO] (Fig. 3*A1*) (18). NL1 KO CA1 pyramidal cells infected in vivo with TKD virus exhibited large deficits in evoked synaptic responses compared with NL1 KO control cells (Fig. 3 *A2* and *A4*). AMPAR EPSCs were reduced by ∼50% (TKD/KO = 115.0 ± 10.8 pA; NL1 KO = 219.8 ± 22.3 pA; TKD/KO = 0.52 ± 0.05 of NL1 KO), whereas in contrast to LRRTM DKD alone (Fig. 2*A*), NMDAR EPSCs were also significantly decreased by ∼25% (TKD/KO = 88.6 ± 15.2 pA; NL1 KO = 117.3 ± 14.9 pA; TKD/KO = 0.76 ± 0.13 of NL1 KO).

The stronger deficits in AMPAR-mediated transmission observed when both LRRTMs and NLs are reduced suggests that these molecules function in a partially redundant manner to recruit or maintain AMPARs at developing synapses. The additional deficit in NMDAR-mediated synaptic responses could reflect either a reduction in the number and/or function of synaptic NMDARs or a reduction in total synapse number. To explore whether in vivo KD of NLs and LRRTMs beginning at P0 alters the total number of synapses, we filled TKD/KO and NL1 KO pyramidal cells with Alexa555-Dextran and imaged spines on secondary dendrites using confocal microscopy (Fig. 3*B*). Al-

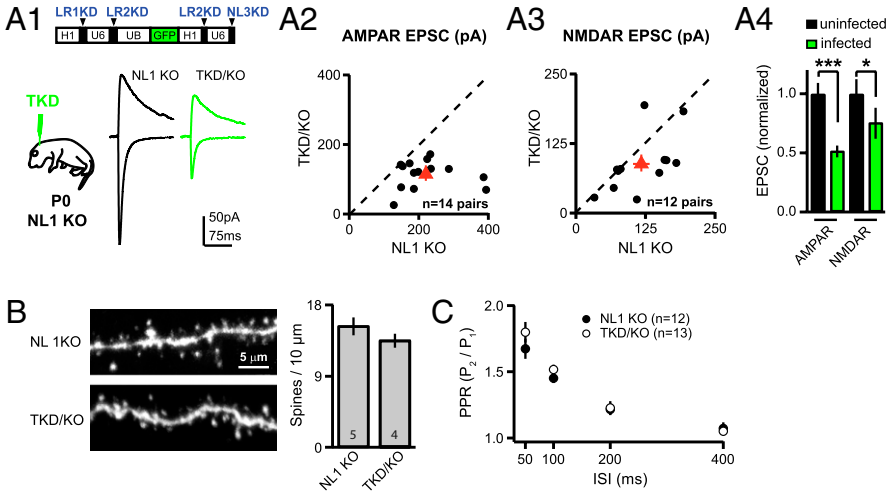

Fig. 3. Functional convergence of NLs and LRRTMs during synaptogenesis. (*A1*) Schematic of vector for TKD of LRRTM1 and -2 and NL3 in P0 NL1 KO mice and representative traces of EPSCs at −60 and +40 mV simultaneously recorded from an uninfected control cell (black) and an infected GFP-expressing cell (green). (*A2* and *A3*) Amplitude of AMPAR and NMDAR EPSCs of infected cells plotted against the amplitudes of simultaneously recorded uninfected controls (black circles) and the average EPSC amplitude (red triangle). (*A4*) Summary graph of AMPAR and NMDAR EPSCs normalized to the average EPSC amplitude of each corresponding uninfected control. (*B Left*) Confocal images of Alexa555 fluorescence of secondary dendrites from fixed NL1 KO and a TKD/KO cell. (*B Right*) Summary of spine density. Numbers within bars represent numbers of neurons analyzed. (*C*) Summary of PPRs measured at the ISIs indicated. All summary values are presented as mean ± SEM. $*P < 0.05$; $***P < 0.001$.

though there was a trend to a decrease in spine density in the cells deficient in NLs and LRRTMs, this trend did not reach statistical significance (NL1 KO = 15.4 ± 2.5 spines/10 μm; TKD/KO = 13.6 ± 1.8 spines/10 μm). These results suggest that, in contrast to cultured neurons (18), acute loss of function of NLs and LRRTMs does not cause massive synapse loss in vivo although these proteins are partially redundant for postsynaptic regulation of excitatory transmission at this early postnatal developmental stage. Because NLs and LRRTMs work cooperatively to maintain postsynaptic function, it is possible that they also cooperate to transynaptically control presynaptic function. However, PPR measurements revealed no differences between TKD/KO and NL1 KO cells at any ISI tested (Fig. 3*C*).

Divergent Functions of NLs and LRRTMs at Mature Synapses in Vivo. To assess the synaptic function of NL1, NL3, and LRRTMs at a time when synaptogenesis is largely complete, we injected WT and NL1 KO mice at P21 with NL3 KD or LRRTM DKD viruses and recorded EPSCs from CA1 pyramidal cells in acute slices at P35–40 (Fig. 4*A*). Because paired recordings from viral infected and adjacent control cells are difficult to obtain from slices of this age, we measured NMDAR/AMPAR ratios to assay changes in synaptic properties. In contrast to the results obtained from P14 to P18 slices (Fig. 1), there was a significant decrease in the NMDAR/AMPAR ratio in the NL1 KO mice compared with WT littermates (Fig. 4*B*) (NL1 KO = 0.76 ± 0.05 of WT). This observation is consistent with previous results and has been attributed to a decrease in the number of synaptic NMDARs (10, 14, 15). NL3 KD in the NL1 KO cells did not further decrease the NMDAR/AMPAR ratio, suggesting that NL1 is the predominant NL for maintaining NMDAR-mediated transmission at mature excitatory CA1 synapses (Fig. 4*B*) (0.77 ± 0.07 of WT). Examination of τ_W of EPSCs at +40 mV at this age (Fig. 4*C*) revealed no differences in NL1 KO or NL1/3 Def cells compared with WT control cells (WT = 81.2 ± 3.4 ms; NL1 KO = 79.8 ± 5.4 ms; NL1/3 Def = 85.4 ± 7.5 ms). Furthermore, the PPRs were not affected by these NL manipulations (Fig. 4*D*).

The use of the constitutive NL1 KO allele precludes us, however, from ruling out a developmental NL1 function that manifests later as deficits in mature transmission. To address this possibility, we generated two bicistronic lentiviral constructs to express NL1 (Fig. 4*E*). One virus only overexpressed NL1 (NL1 O/E), whereas the second virus also contained the shRNA to NL3 (NL3 KD + NL1). Western blot analysis showed that both constructs effectively drive NL1 expression above endogenous levels in cultured neurons. Expression of NL1 with the shRNA to NL3 in NL1 KO mice reversed the NMDAR/AMPAR ratio phenotype observed in NL1 KO mice (Fig. 4*F*) (NL1/3 Def + NL1 = 1.2 ± 0.06 of WT), whereas overexpression of NL1 in WT mice yielded NMDAR/AMPAR ratios that were no different from WT ratios (Fig. 4*F*) (NL1 O/E = 1.2 ± 0.15 of WT). These results show that NL1 functions to maintain NMDAR-mediated transmission at mature synapses.

To test whether LRRTMs also play a role in regulating excitatory synaptic transmission at mature synapses, we injected the LRRTM DKD lentivirus into the hippocampal CA1 layer of WT mice. This manipulation did not significantly change the NMDAR/AMPAR ratio compared with WT cells (Fig. 4*G*) (LRRTM DKD = 1.17 ± 0.08 of WT). In addition, PPRs were not affected by the LRRTM DKD (Fig. 4*H*). Although these results suggest that the functional roles of NLs and LRRTMs at mature synapses differ, they still may functionally compensate for one another in a manner similar to the manner observed during the first 2 postnatal wk (Fig. 3). To test this possibility, we injected the TKD lentivirus into the hippocampus of NL1 KO mice and measured NMDAR/AMPAR ratios. This manipulation did not have any additional effect on these measurements compared with those effects obtained from NL1 KO cells (Fig.4*I*) (TKD/KO = 1.07 ± 0.11 of NL1 KO). Together, these results suggest that LRRTMs do not play a major role in regulating basal synaptic transmission at mature excitatory CA1 synapses.

A limitation of these experiments is that the NMDAR/AMPAR ratios used to assess basal synaptic properties will not change if the number of synapses per cell has changed as long as the average properties of individual synapses remain constant. It is, therefore, possible that the KD of NLs and LRRTMs caused a loss in the total number of synapses, which was observed in dissociated cultured neurons (18). To address this possibility, we filled cells with Alexa555-Dextran and examined dendritic spine density and morphology (Fig. 4*J*). Spine density in TKD/KO cells was not significantly different from the density in NL1 KO controls (NL1 KO = 16.5 ± 0.8 spines/10 μm; TKD/KO = 15.8 ± 1.2 spines/10 μm). Furthermore, visual classification of the relative proportion of spines with different morphologies (mushroom, stubby, and filopodia) (25) revealed no differences in the TKD/KO cells (NL1 KO = 72.8 ± 1.4% mushroom, 25.7 ± 1.7% stubby, and 1.6 ± 0.3% filopodia; TKD/KO = 71.5 ± 2.8% mushroom, 27.3 ± 2.9% stubby, and 1.1 ± 0.4% filopodia). Finally, quantitative estimates of spine head area also revealed no effects. Thus, in vivo, normal levels of NLs and LRRTMs are not required for the maintenance of spine density and morphology, and therefore, presumably, are not required for the maintenance of normal mature synapse structure.

Extracellular Domains of LRRTMs and NLs Are Sufficient to Reverse Transmission Deficits. Several families of PDZ domain-containing proteins, most notably the membrane-associated guanylate kinases (MAGUKs), are important for recruiting and/or maintaining synaptic AMPARs and NMDARs (26, 27). Both NLs and

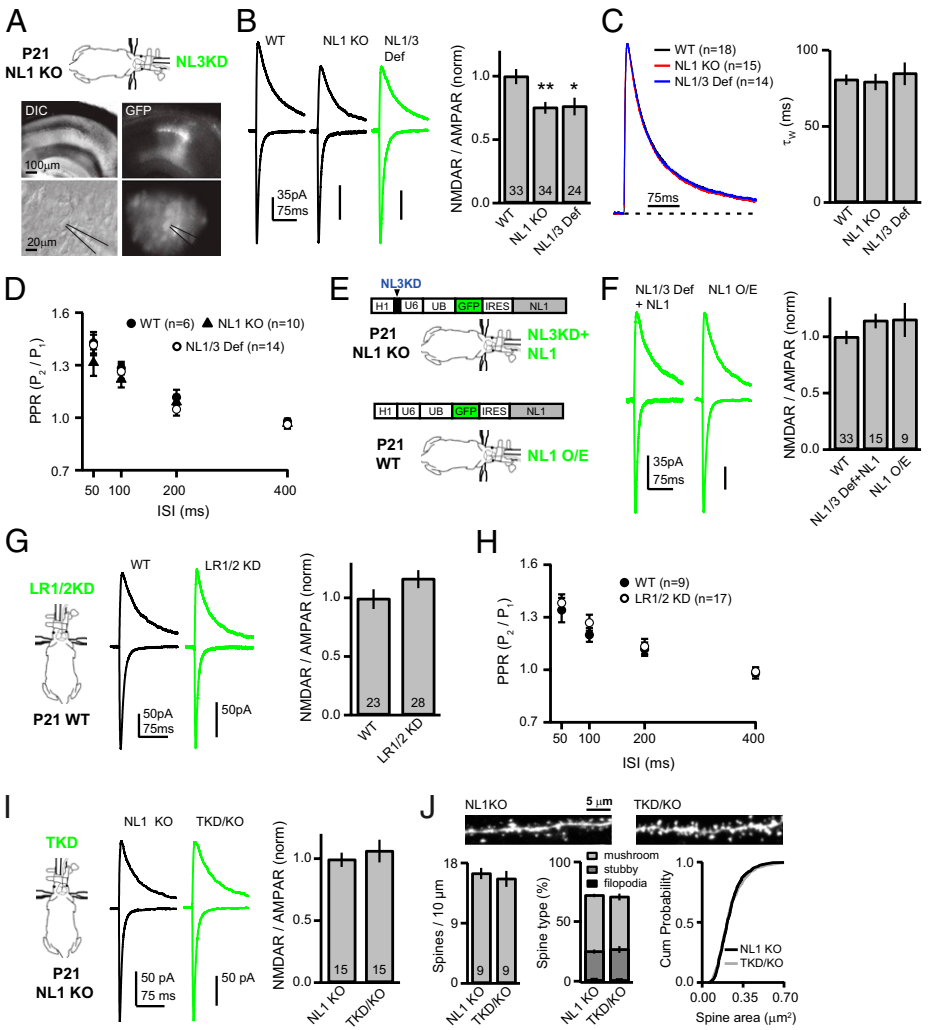

Fig. 4. Functional divergence of NLs and LRRTMs at mature synapses. (*A Top*) Schematic representing stereotactic injection of the NL3 KD virus into a P21 NL1 KO mouse. All subsequent panels where this diagram appears are represented in the same manner: In black, the mouse's genotype is shown, and in green, the lentivirus injected is shown. (*A Middle*) Screen captures of a hippocampal slice in differential interference contrast (DIC) (*A Middle Left*) and epifluorescence (*A Middle Right*) showing localized CA1 infection. (*A Bottom*) Capture showing magnified single cells infected within the CA1 layer. Black lines outline a patch electrode. (*B*) Sample currents recorded at −60 and +40 mV (*B Left*), and the summary of NMDAR/AMPAR ratios normalized to WT (*B Right*). (*C Left*) Average normalized EPSCs recorded at +40 mV from WT (black), NL1KO (red), and NL1/3 Def (blue) neurons. Solid lines are averages across multiple cells (indicated by the numbers in parentheses), and shaded areas represent the SEM. (*C Right*) Summary of the weighted decay time constant obtained from double exponential fits to each individual experiment. (*D*) Summary of PPRs measured at four different ISIs from cells of the indicated genotypes. (*E*) Schematic of the NL1 rescue and O/E constructs. (*F*) Sample EPSCs (*F Left*) and summary graph of NMDAR/AMPAR ratios normalized to WT (*F Right*) from neurons infected with the indicated viruses. (*G*) The same as in *F* for experiments using the LRRTM DKD virus injected into P21 WT mice. (*H*) Summary of PPRs measured at the ISIs indicated for WT and LRRTM DKD cells. (*I*) The same as in *F* for experiments using the TKD virus injected into P21 NL1 KO mice. (*J Upper*) Confocal images of Alexa555 fluorescence of secondary dendrites from cells of the indicated genotypes. (*J Lower*) Analysis of spine density, morphological classification, and spine head area (represented as cumulative distribution) for the indicated genotypes. In all cases, summary values are represented as mean ± SEM. $^{*}P < 0.05$; $^{**}P < 0.01$.

LRRTMs contain short intracellular tails that include a C-terminal PDZ domain binding sequence (11, 28), suggesting that these sequences may also be required for their influence on excitatory synaptic transmission. Alternatively, NLs and LRRTMs may subserve their synaptic functions independent of MAGUKs, relying primarily on their extracellular interactions with NRXs or as yet unknown synaptic adhesion molecules. To address this issue, we generated lentiviruses that express LRRTM2 or NL1 without their intracellular domains (Fig. 5) (LRRTM DKD + LRRTM2-EC and NL3KD + NL1-EC, respectively). Because the LRRTM DKD induces a specific reduction in AMPAR-mediated transmission at developing synapses (Fig. 2*A2*), we injected LRRTM DKD + LRRTM2-EC viruses into P0 WT mice and performed paired recordings (Fig. 5*A1*). Replacement of LRRTM1 and LRRTM2 with the extracellular domain of LRRTM2 reversed the reduction in AMPAR-mediated synaptic currents observed in LRRTM DKD cells (Fig. 5 *A2* and *A4*) (WT = 139.9 ± 13.8 pA; LRRTM DKD + LRRTM2-EC = 121.7 ± 13.2 pA; LRRTM DKD + LRRTM2-EC = 0.87 ± 0.09 of WT) but had no effect on NMDAR-mediated synaptic currents (Fig. 5 *A3* and *A4*) (LRRTM DKD + LRRTM2-EC = 80.4 ± 6.5 pA; WT = 84.8 ± 8.6 pA; LRRTM DKD + LRRTM2-EC = 0.95 ± 0.08 of WT).

To determine if NL1 behaves similarly to LRRTM2, we injected NL3 KD + NL1-EC into NL1 KO mice at P21 (Fig. 5*B*), the time at which NLs function to maintain NMDAR-mediated transmission. This manipulation increased the NMDAR/AMPAR ratio to WT levels (Fig. 5*B*) (NL1/3 Def + NL1-EC = 1.07 ± 0.06 of WT), a significantly higher ratio compared with NL1 KO cells. These results indicate that the intracellular sequence of LRRTM2 is not required for recruiting and/or stabilizing AMPARs at developing synapses, consistent with the finding that these sequences are also not required for increasing the synapse density of cultured neurons on overexpression of LRRTM or NL1 (18). Similarly, the intracellular sequence of NL1 is not essential to maintain NMDAR-mediated synaptic responses.

Discussion

NRXs, NLs, and LRRTMs comprise part of a transsynaptic protein interaction network that is ideally positioned to play important roles in the development, maintenance and function of synapses. To explore the in vivo synaptic roles of NLs and LRRTMs, we have taken a systematic loss of function approach using lentiviral KD and comparing two developmental time points. We found that during the first 2 wk of postnatal development, KO of NL1 and KD of NL3, did not alter net excitatory synaptic transmission or synapse numbers. In contrast, KD of LRRTMs at this time point led to a specific decrease in AMPAR-mediated transmission. Consistent with functional compensation during early postnatal development, KD of LRRTM1 and LRRTM2 along with NL3 in NL1 KO mice caused a substantially larger decrease in excitatory transmission,

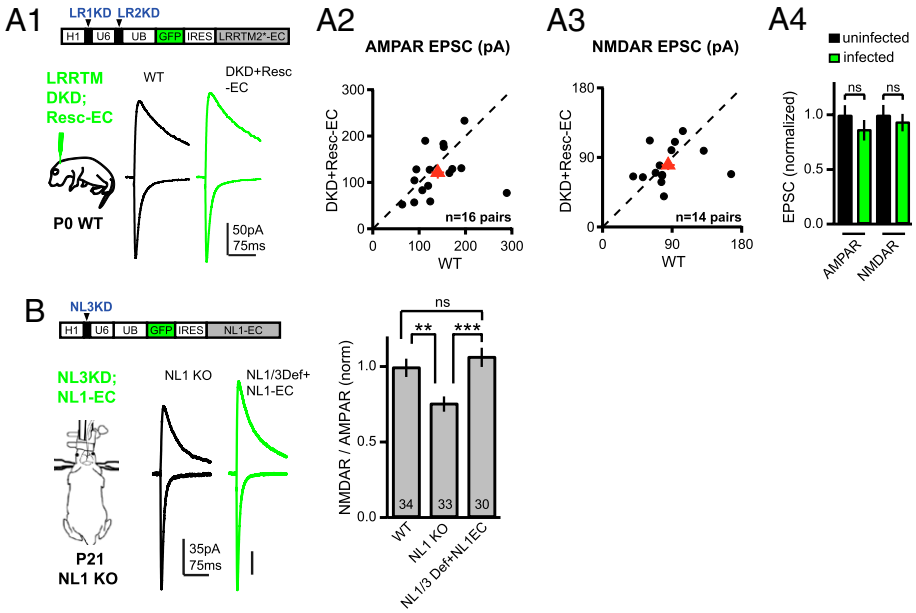

Fig. 5. The extracellular domains of LRRTM2 and NL1 are sufficient to rescue the KD-induced synaptic deficits. (*A1*) Schematic of rescue vector expressing the extracellular domain of LRRTM2 in P0 WT mice with representative traces of EPSCs at −60 and +40 mV simultaneously recorded from an uninfected control (black) and an infected GFP-expressing cell (green). (*A2* and *A3*) Amplitude of AMPAR and NMDAR EPSCs of infected cells plotted against the amplitudes of simultaneously recorded uninfected controls (black circles) and the average EPSC amplitude (red triangle). (*A4*) Summary graph of AMPAR and NMDAR EPSCs normalized to the average EPSC amplitude of each corresponding uninfected control. (*B*) Schematic of the rescue vector used to express the extracellular domain of NL1, sample traces of EPSCs, and summary graph of NMDAR/AMPAR ratios normalized to WT from neurons infected with the indicated virus. WT and NL1 KO data were shown in Fig. 4 and are replotted here for comparison. In all cases, summary values are represented as mean ± SEM. $^{**}P < 0.01$; $^{***}P < 0.001$.

with both the AMPAR- and NMDAR-mediated components being affected. Strikingly, the density of synapses, defined by the density of postsynaptic spines on dendrites, was unaffected by LRRTM/NL deficiency (Fig. 3*B*), suggesting that LRRTMs and NLs function cooperatively at developing synapses to recruit or maintain AMPARs and to a lesser extent, NMDARs. Importantly, the relative functions of NLs and LRRTMs seem to change as synapses mature. Manipulation of NL1 and NL3 at P21–35 led to decreased NMDAR-mediated transmission, whereas KD of LRRTM1 and LRRTM2 did not have detectable effects. Furthermore, in contrast to the synaptogenic period during the first 2 postnatal wk, we found no functional compensation between the two families of NRX ligands at mature synapses. The deficits in synaptic transmission caused by the NL loss of function at mature synapses were not accompanied by changes in synapse numbers or spine morphology. Together, these results show a functionally dynamic synaptic cell adhesion network, with NLs and LRRTMs having both overlapping and unique functions that change during postnatal development.

A principle limitation of the present study, imposed by the currently available tools and shared by all other studies to date, is that the manipulations that we used either do not cause a complete loss of the target protein (as in the case for NL3 and LRRTM KDs) or are present throughout development (as in the case of the NL1 KO). Another limitation is that, although the KDs that we used were well-validated in cultured neurons and off-target effects were excluded (18), it is formally possible that the efficacy and specificity of these KDs in vivo may differ.

Removal of NRX Ligands During Synaptogenesis. NL1 and NL3 loss of function during a major period of synaptogenesis elicited no significant change in global excitatory synaptic strength as measured by paired recordings. This result is consistent with previous work showing maintenance of normal synapse numbers in NL1/2/3 triple KO mice (13) and the lack of effect of performing identical manipulations with the same viruses on excitatory synapse density in dissociated cultured neurons (18). However, this result is not consistent with several other studies (Table S1 shows a summary). In particular, a recent study using microRNA-mediated simultaneous KD of NL1-3 caused a robust reduction of both AMPAR- and NMDAR-mediated currents as well as synapse density in rat slice culture preparations (12). Because of the many differences in the methodologies and preparations used, it is difficult to directly compare these observations with the lack of effect that we observed when NL3 was reduced in vivo both in WT and NL1 KO backgrounds and assayed in acute slices. NL1-3 microRNA expression was initiated 1 d after preparation of the organotypic slice cultures (12), a period marked by massive circuit reorganization that includes concomitant synapse retraction and synaptogenesis. Thus, the KD of NL1-3 under these conditions may both accelerate synapse loss and impair subsequent reestablishment of synaptic connections in a manner that does not normally occur in vivo. Moreover, KD of NL1-3 in this slice culture preparation caused a large decrease in inhibitory synaptic transmission, an effect that could lead to a decrease in excitatory synaptic function as a result of homeostatic compensation to preserve the net excitatory/inhibitory balance (29). Finally, as is the case for any study using RNAi, it is possible that one or more of the microRNAs has some nonspecific effect, a possibility that is difficult to rule out using a rescue approach, because overexpression of either NL1 or NL3 alone caused robust gain of function phenotypes in this preparation. Thus, the rescue may not actually correct the loss of function but rather, be a reversal of a phenotype that was because of an off-target effect. Moreover, it is possible that, in vivo, other families of postsynaptic cell adhesion molecules may have compensated for the lack of NL1 and NL3 during early postnatal development (see below), although this hypothesis is difficult to reconcile with the synaptic phenotypes that the NL1 KO produces (10).

The specific effect of the LRRTM1 and LRRTM2 DKD on AMPAR-mediated transmission in CA1 pyramidal cells during the same early postnatal time period suggests that LRRTMs support AMPAR recruitment to synapses and/or their maintenance at synapses. This result, however, contrasts with the report that LRRTM2 KD alone in P6 dentate gyrus granule cells caused large matching decreases in both AMPAR- and NMDAR-mediated synaptic currents (6). This large suppression of excitatory transmission is surprising given that mRNAs of all four LRRTM family members are robustly expressed in this cell type (20). One potential explanation for this discrepancy is that the shRNA to LRRTM2 used in this previous study had off-target effects. Although a rescue with WT LRRTM2 was successfully obtained in cultured neurons expressing this shRNA, this result does not rule out off-target effects, because LRRTM2 has dramatic synaptogenic effects when overexpressed in neuronal cultures (5, 6). Indeed, we confirmed that the shRNA to LRRTM2 used previously (6) decreases synapse density in dissociated hippocampal cultures but also found that two other equally effective shRNAs to LRRTM2 did not (18), findings that are consistent with an off-target effect of the initial LRRTM2 shRNA.

The synaptic deficit elicited by LRRTM1 and LRRTM2 KD in vivo was significantly increased by simultaneous KO/KD of NL1 and NL3. This result suggests that these proteins are functionally redundant during early postnatal developmental, a conclusion that is in keeping with the striking similarity of the binding of both ligands to NRXs, despite the absence of any structural similarity (5–7). One important difference between the effects of simultaneous KD of NL3, LRRTM1, and LRRTM2 in NL1 KO neurons in culture (18) vs. in vivo was that no change in synapse density was detected after the in vivo manipulations. This difference in results may highlight an important inherent difference in the state of in vitro vs. in vivo synapses regarding their susceptibility to activity-dependent pruning. Because identical viruses were used for both the in vitro experiments in culture and the in vivo injections, this difference also strongly suggests that neuronal and synaptic properties in cultured neurons cannot automatically be assumed to translate to neurons and synapses in vivo. It should be noted, however, that the general approach pursued here—shRNA-dependent KD of targets—carries the inherent limitation that most shRNAs, such as the ones that we use here, exert KDs of 70–90% and that no shRNA produces a complete KD. The remaining expression of the target proteins may mediate significant functional effects. Thus, when performing shRNA-mediated KD in small numbers of individual cells, it is impossible to know the quantitative effectiveness of the KD and therefore, impossible to rule out that identical shRNAs expressed using the same batch of viruses are, for some reason, less effective in vivo than in vitro.

Role of NLs and LRRTMs at Mature Synapses. A major advantage of the in vivo approach that we have taken is that the function of NLs and LRRTMs at mature synapses could be studied in the absence of developmental synaptogenesis. Our results suggest that, at mature synapses, NLs and LRRTMs subserve different functions than at developing synapses. NL1 is essential for the regulation of NMDAR-mediated synaptic responses, consistent with findings based on recordings from hippocampal pyramidal neurons in slices prepared from NL1 KO mice (10) and amygdala principle neurons on acute KD of NL1 (14, 15). We have extended these results in two ways. First, we show that NL1 and NL3 are not required for the initial recruitment of NMDARs to postnatal developing synapses. Second, our rescue experiments in NL1 KO mice show that NL1 is actively required at mature synapses for the maintenance of NMDAR-mediated transmission. In contrast to the effect of the loss of function of NLs, KD of LRRTM1 and LRRTM2 had no detectable effects on NMDAR/AMPAR ratios obtained from P35 to P40 slices. Furthermore, KD of both NLs and LRRTMs beginning at P21 had no significant effects on spine density or spine morphology.

There are several possible interpretations of these results. We cannot rule out that the remaining levels of these NRX ligands at individual synapses in vivo were still functionally sufficient. This caveat, of course, applies to all negative results obtained using KD approaches. It is also possible that larger functional and structural effects may not have occurred after the molecular manipulations because of homeostatic compensatory synaptic adaptations. This caveat applies to both constitutive KOs and more acute KD approaches. We favor the conclusion that LRRTMs do not play a role in regulating basal synaptic transmission at mature synapses, and neither LRRTMs nor NLs is required for maintaining normal spine structure. Given their ability to maintain or recruit AMPARs at developing synapses and their persistence expression at mature synapses, LRRTMs may instead play a role in activity-dependent synaptic phenomena (18), an exciting possibility that remains to be tested in vivo.

Both NLs and LRRTMs contain intracellular tails capable of binding scaffolding modules and intracellular signaling proteins as well as large extracellular domains that bridge the synaptic cleft. Surprisingly, we found that the extracellular domain of LRRTM2 alone is sufficient to reverse the deficit in AMPAR-mediated transmission elicited by the LRRTM DKD. Confidence in this result is increased by the parallel finding that the extracellular domain of LRRTM2 is sufficient to reverse the synapse loss caused by TKD of LRRTM1, LRRTM2, and NL3 in NL1 KO cultured neurons (18). Possible hypotheses to explain these results include direct interaction of the extracellular domain of LRRTMs with AMPARs (6), indirect *cis* interactions with a mediator protein, and indirect *trans* interactions, where NRXs dictate the localization of AMPARs. In a similar fashion, replacement of NL1 and NL3 deficient synapses with the extracellular sequence of NL1 completely rescued the reduced NMDAR/AMPAR ratio as effectively as full-length NL1. Although it is impossible to rule out that the small amounts of remaining endogenous LRRTMs or NL3 in the KD cells were sufficient to heterodimerize with the overexpressed mutant forms of recombinant LRRTM2 and NL3 and thus, provide intracellular domains that were critical for the functional rescues that we observed, this explanation seems unlikely given the relative amounts of the endogenous and recombinant proteins. Instead, we favor the hypothesis that the extracellular domains of these neurexin binding proteins are critically important not only for their synaptogenic effects but also for their effects on synaptic function.

Complexity of Neuroligin and LRRTM Function. Neuroligins, and more recently, LRRTMs have been the object of intense interest, in large part because of their ubiquitous presence at synapses and their genetic association with a number of neuropsychiatric disorders. Examining their function is challenging, because there are multiple isoforms of each (NL1–4 and LRRTM1–4) and all of the isoforms exhibit high affinity for neurexins, although their affinities differ depending on splice variants and neurexin isoforms. Table S1 presents an attempt at a concise yet comprehensive summary of the studies that have molecularly manipulated NLs or LRRTMs in neurons and performed assays of synapse number or function. The results are confusing and likely reflect not only the inherent complexity of the synaptic functions of these NRX ligand protein families but also the differences in approaches used and the inherent limitations of each approach. Nevertheless, several tentative general conclusions can be reached. First, when overexpressed in cultured neurons, NLs and LRRTMs routinely increase synapse numbers. However, as is the case with any overexpressed protein, there is the potential for mistargeting, which may yield nonphysiological abnormal or even dominant positive or negative effects. Furthermore, the limited results to date suggest that the robust synaptogenic effects of overexpressing NLs and LRRTMs in cultured neurons may not occur in vivo, although they do seem to operate in cultured slices.

Second, although it is an extremely powerful approach, using RNAi always raises the confound of off-target effects and partial loss of function results. Off-target effects may explain some of the profound differences in the synaptic deficits reported to be caused by shRNAs targeting single NLs or LRRTMS in cultured neurons as well as the differences between the reported effects of RNAi-mediated KD of NLs vs. the relatively modest effects caused by genetic deletion of NLs. Rescue experiments that reverse the synaptic phenotype caused by KD manipulations are valuable in minimizing the possibility that off-target effects caused the observed synaptic changes but are not foolproof if overexpression of the recombinant protein alone yields a gain of function phenotype. In this latter case, a rescue may actually reflect a reversal or masking of the synaptic changes caused by the shRNA.

Third, as mentioned above, the preparation in which molecular manipulations are performed may significantly influence the synaptic effects that are observed. Dissociated neuronal and slice culture preparations are valuable because of the relative access that they provide, but their synapses may not accurately reflect the state of synapses in vivo, especially if the molecular manipulation is performed at a time when robust synaptogenesis and synaptic pruning are occurring.

Fourth, the NL and LRRTM protein families likely have both redundant and distinct synaptic functions. As shown here, their specific roles also will depend on the maturational state of the

synapses in which they are localized and the specific circuit in which the synapses function (30).

In summary, to test and extend the work on the synaptic functions of the two NRX ligands NLs and LRRTMs, we have examined the in vivo synaptic effects of molecular manipulations of these proteins. Although our results indicate that NLs and LRRTMs can partly functionally compensate for each other early during development, they also suggest that these cell adhesion molecules perform distinct functions at mature excitatory synapses in that they independently regulate AMPAR- and NMDAR-mediated synaptic transmission. Numerous human genetics studies implicate NRXs, NLs, and LRRTMs in the pathogenesis of various neuropsychiatric disorders, including autism and schizophrenia (reviewed in ref. 31). Additional elucidation of their detailed functions in vivo will, therefore, be crucial not only for a more sophisticated understanding of normal synapse development, function, and plasticity but also for how synaptic dysfunction can lead to disease.

Materials and Methods

Lentiviral Expression Vectors. For details of lentivirus vectors and production, see *SI Materials and Methods*.

Hippocampus Infection. All mice used in this study are F1 hybrids of C57/B6 and 129SVE (Charles River). Animals were handled in accordance with Stanford and Federal Guidelines. Injections (P0 and P21 mice) were performed through glass pipettes using an infusion pump (Harvard Apparatus). P0 pups were anesthetized for 2 min in ice and placed in a custom-made pedestal. Concentrated lentiviruses (500 nL) were infused transcranially into the hippocampus at a rate of 800 nL/min. Stereotaxic injections into P21 mice (10–12 g) were performed as previously described (33).

Slice Preparation and Whole-Cell Recordings. Mice (postnatal days 14–18 or 35–39) were decapitated after deep isoflurane anesthesia. The brain was removed and placed in ice-cold media consisting of 228 mM sucrose, 26 mM $NaHCO_3$, 11 mM glucose, 7.0 mM $MgSO_4$, 2.5 mM KCl, 1.0 mM NaH_2PO_4, and 0.5 mM $CaCl_2$. Horizontal slices were cut in 225-μm-thick sections using a vibratome (VT1200S; Leica) and transferred to an incubation chamber containing artificial cerebrospinal fluid consisting of 122 mM NaCl, 26 mM $NaHCO_3$, 11 mM glucose, 2.5 mM $CaCl_2$, 2.5 mM KCl, 1.3 mM $MgCl_2$, and 1.0 mM NaH_2PO4. Slices were incubated for 45–60 min at 32 °C and then kept at room temperature until transfer to a submerged recording chamber perfused with artificial cerebrospinal fluid (28–30 °C) containing picrotoxin (50 μM; Sigma). Whole-cell recordings from CA1 pyramidal neurons were obtained with patch electrodes containing 117.5 mM cesium methanesulfonate, 15.5 mM CsCl, 10 mM TEA-Cl, 10 mM Hepes buffer, 10 mM sodium phosphocreatine, 8 mM NaCl, 5 mM EGTA, 1 mM $MgCl_2$, 4 mM Mg-ATP, 0.3 mM Na-GTP, and 1 mM QX-314. Electrode resistances ranged from 2.5 to 4.5 MΩ. Simultaneous dual whole-cell recordings (P14–18 experiments) were obtained from infected and adjacent uninfected cells (indicated by GFP expression or lack thereof) (Fig. S1). In experiments where dual recordings were not feasible (P35–40), a recording from a control cell was made in each slice from which a GFP-expressing cell was recorded. EPSCs were evoked by brief current injections (10–50 μA and 0.2 ms) delivered to Schaffer collaterals (0.1 Hz) through electrodes made from θ-glass (Warner).

Data Acquisition and Analysis. EPSCs were recorded in whole-cell voltage clamp (Multiclamp 700B; Molecular Devices), filtered at 4 KHz, and digitized at 10 KHz (ITC-18 interface; HEKA). Electrophysiological data were acquired and analyzed using the Recording Artist package (Rick Gerkin) written in Igor Pro (Wavemetrics). AMPAR (−60 mV) and NMDAR (+40 mV) EPSCs were obtained by averaging 20–30 consecutive responses. The AMPAR EPSC amplitude was measured within a 2-ms window around the peak, whereas the NMDAR EPSC amplitude was measured as the average current 49–51 ms after the stimulus. PPR curves were generated as previously described (34). The weighted decay time constant (τ_W) of EPSCs at +40 mV was calculated by fitting a double exponential function to the average EPSC for each cell and using the following formula: $\tau_W = [(A_1 \times \tau_1) + (A_2 \times \tau_2)]/(A_1 + A_2)$, where A_1 and A_2 are the amplitudes and τ_1 and τ_2 are the decay time constants of the fast and slow components, respectively. Summary data are presented as mean ± SEM unless otherwise stated. Comparison between infected and uninfected cell responses resulting from paired recordings was done using paired, two-tailed Student *t* test. All other statistical analyses were done using unpaired, two-tailed *t* test. Differences were considered significant if $P < 0.05$.

Tissue Fixation and Microscopy. For details, see *SI Materials and Methods*.

ACKNOWLEDGMENTS. We thank Dr. Daniela Ion for assistance with stereotactic injections. This work was supported by National Institute of Mental Health Grant MH086176-02 (to M.V.F.), International Human Frontier Science Program Organization Grant LT00021/2008-L (to J.K.), and grants from the National Institute of Mental Health (to T.C.S. and R.C.M.) and Simons Foundation (to T.C.S.).

1. Ichtchenko K, et al. (1995) Neuroligin 1: A splice site-specific ligand for beta-neurexins. *Cell* 81:435–443.
2. Ushkaryov YA, Petrenko AG, Geppert M, Südhof TC (1992) Neurexins: Synaptic cell surface proteins related to the alpha-latrotoxin receptor and laminin. *Science* 257:50–56.
3. Boucard AA, Chubykin AA, Comoletti D, Taylor P, Südhof TC (2005) A splice code for trans-synaptic cell adhesion mediated by binding of neuroligin 1 to alpha- and beta-neurexins. *Neuron* 48:229–236.
4. Chih B, Gollan L, Scheiffele P (2006) Alternative splicing controls selective trans-synaptic interactions of the neuroligin-neurexin complex. *Neuron* 51:171–178.
5. Ko J, Fuccillo MV, Malenka RC, Südhof TC (2009) LRRTM2 functions as a neurexin ligand in promoting excitatory synapse formation. *Neuron* 64:791–798.
6. de Wit J, et al. (2009) LRRTM2 interacts with Neurexin1 and regulates excitatory synapse formation. *Neuron* 64:799–806.
7. Siddiqui TJ, Pancaroglu R, Kang Y, Rooyakkers A, Craig AM (2010) LRRTMs and neuroligins bind neurexins with a differential code to cooperate in glutamate synapse development. *J Neurosci* 30:7495–7506.
8. Scheiffele P, Fan J, Choih J, Fetter R, Serafini T (2000) Neuroligin expressed in nonneuronal cells triggers presynaptic development in contacting axons. *Cell* 101:657–669.
9. Chih B, Engelman H, Scheiffele P (2005) Control of excitatory and inhibitory synapse formation by neuroligins. *Science* 307:1324–1328.
10. Chubykin AA, et al. (2007) Activity-dependent validation of excitatory versus inhibitory synapses by neuroligin-1 versus neuroligin-2. *Neuron* 54:919–931.
11. Linhoff MW, et al. (2009) An unbiased expression screen for synaptogenic proteins identifies the LRRTM protein family as synaptic organizers. *Neuron* 61:734–749.
12. Shipman SL, et al. (2011) Functional dependence of neuroligin on a new non-PDZ intracellular domain. *Nat Neurosci* 14:718–726.
13. Varoqueaux F, et al. (2006) Neuroligins determine synapse maturation and function. *Neuron* 51:741–754.
14. Kim JH, et al. (2008) Neuroligin-1 is required for normal expression of LTP and associative fear memory in the amygdala of adult animals. *Proc Natl Acad Sci USA* 105:9087–9092.
15. Jung S-Y, et al. (2010) Input-specific synaptic plasticity in the amygdala is regulated by neuroligin-1 via postsynaptic NMDA receptors. *Proc Natl Acad Sci USA* 107:4710–4715.
16. Missler M, et al. (2003) Alpha-neurexins couple Ca^{2+} channels to synaptic vesicle exocytosis. *Nature* 423:939–948.
17. Elias GM, et al. (2006) Synapse-specific and developmentally regulated targeting of AMPA receptors by a family of MAGUK scaffolding proteins. *Neuron* 52:307–320.
18. Ko J, Soler-Llavina GJ, Fuccillo MV, Malenka RC, Südhof TC (2011) Neuroligins/LRRTMs prevent activity- and Ca^{2+}/calmodulin-dependent synapse elimination in cultured neurons. *J Cell Biol* 194:323–334.
19. Song JY, Ichtchenko K, Südhof TC, Brose N (1999) Neuroligin 1 is a postsynaptic cell-adhesion molecule of excitatory synapses. *Proc Natl Acad Sci USA* 96:1100–1105.
20. Laurén J, Airaksinen MS, Saarma M, Timmusk T (2003) A novel gene family encoding leucine-rich repeat transmembrane proteins differentially expressed in the nervous system. *Genomics* 81:411–421.
21. Budreck EC, Scheiffele P (2007) Neuroligin-3 is a neuronal adhesion protein at GABAergic and glutamatergic synapses. *Eur J Neurosci* 26:1738–1748.
22. Varoqueaux F, Jamain S, Brose N (2004) Neuroligin 2 is exclusively localized to inhibitory synapses. *Eur J Cell Biol* 83:449–456.
23. Sheng M, Cummings J, Roldan LA, Jan YN, Jan LY (1994) Changing subunit composition of heteromeric NMDA receptors during development of rat cortex. *Nature* 368:144–147.
24. Bellone C, Nicoll RA (2007) Rapid bidirectional switching of synaptic NMDA receptors. *Neuron* 55:779–785.
25. Sorra KE, Harris KM (2000) Overview on the structure, composition, function, development, and plasticity of hippocampal dendritic spines. *Hippocampus* 10:501–511.
26. Scannevin RH, Huganir RL (2000) Postsynaptic organization and regulation of excitatory synapses. *Nat Rev Neurosci* 1:133–141.
27. Elias GM, Nicoll RA (2007) Synaptic trafficking of glutamate receptors by MAGUK scaffolding proteins. *Trends Cell Biol* 17:343–352.
28. Irie M, et al. (1997) Binding of neuroligins to PSD-95. *Science* 277:1511–1515.
29. Turrigiano GG (2008) The self-tuning neuron: Synaptic scaling of excitatory synapses. *Cell* 135:422–435.
30. Etherton M, et al. (2011) Autism-linked neuroligin-3 R451C mutation differentially alters hippocampal and cortical synaptic function. *Proc Natl Acad Sci USA* 108:13764–13769.
31. Südhof TC (2008) Neuroligins and neurexins link synaptic function to cognitive disease. *Nature* 455:903–911.
32. Pang ZP, Cao P, Xu W, Südhof TC (2010) Calmodulin controls synaptic strength via presynaptic activation of calmodulin kinase II. *J Neurosci* 30:4132–4142.
33. Cetin A, Komai S, Eliava M, Seeburg PH, Osten P (2006) Stereotaxic gene delivery in the rodent brain. *Nat Protoc* 1:3166–3173.
34. Carter AG, Soler-Llavina GJ, Sabatini BL (2007) Timing and location of synaptic inputs determine modes of subthreshold integration in striatal medium spiny neurons. *J Neurosci* 27:8967–8977.